JOURNAL OF GEOPHYSICAL RESEARCH, VOL. 107, NO. D20, 8276, doi:10.1029/2001JD000533, 2002

Chemical depletion of Arctic ozone in winter 1999/2000

M. Rex,[1] R. J. Salawitch,[2] N. R. P. Harris,[3] P. von der Gathen,[1] G. O. Braathen,[4] A. Schulz,[1] H. Deckelmann,[1] M. Chipperfield,[5] B.-M. Sinnhuber,[5] E. Reimer,[6] R. Alfier,[6] R. Bevilacqua,[7] K. Hoppel,[7] M. Fromm,[8] J. Lumpe,[8] H. Küllmann,[9] A. Kleinböhl,[9] H. Bremer,[9] M. von König,[9] K. Künzi,[9] D. Toohey,[10] H. Vömel,[11] E. Richard,[12] K. Aikin,[12] H. Jost,[13] J. B. Greenblatt,[13] M. Loewenstein,[13] J. R. Podolske,[13] C. R. Webster,[2] G. J. Flesch,[2] D. C. Scott,[2] R. L. Herman,[2] J. W. Elkins,[12] E. A. Ray,[12] F. L. Moore,[12] D. F. Hurst,[12] P. Romashkin,[12] G. C. Toon,[2] B. Sen,[2] J. J. Margitan,[2] P. Wennberg,[14] R. Neuber,[1] M. Allart,[15] B. R. Bojkov,[4] H. Claude,[16] J. Davies,[17] W. Davies,[18] H. De Backer,[19] H. Dier,[20] V. Dorokhov,[21] H. Fast,[17] Y. Kondo,[22,23] E. Kyrö,[24] Z. Litynska,[25] I. S. Mikkelsen,[26] M. J. Molyneux,[27] E. Moran,[28] T. Nagai,[29] H. Nakane,[30] C. Parrondo,[31] F. Ravegnani,[32] P. Skrivankova,[33] P. Viatte,[34] and V. Yushkov[21]

Received 12 February 2001; revised 2 July 2001; accepted 7 July 2001; published 20 September 2002.

[1] During Arctic winters with a cold, stable stratospheric circulation, reactions on the surface of polar stratospheric clouds (PSCs) lead to elevated abundances of chlorine monoxide (ClO) that, in the presence of sunlight, destroy ozone. Here we show that PSCs were more widespread during the 1999/2000 Arctic winter than for any other Arctic winter in the past two decades. We have used three fundamentally different approaches to derive the degree of chemical ozone loss from ozonesonde, balloon, aircraft, and satellite instruments. We show that the ozone losses derived from these different instruments and approaches agree very well, resulting in a high level of confidence in the results. Chemical processes led to a 70% reduction of ozone for a region ~1 km thick of the lower stratosphere, the largest degree of local loss ever reported for the Arctic. The Match analysis of ozonesonde data shows that the accumulated chemical loss of ozone inside the Arctic vortex totaled 117 ± 14 Dobson units (DU) by the end of winter. This loss, combined with dynamical redistribution of air parcels, resulted in a 88 ± 13 DU reduction in total column ozone compared to the amount that would have been present in the

[1]Alfred Wegener Institute for Polar and Marine Research, Potsdam, Germany.
[2]Jet Propulsion Laboratory, California Institute of Technology, Pasadena, California, USA.
[3]European Ozone Research Coordinating Unit, University of Cambridge, Cambridge, UK.
[4]Norsk Institutt for Luftforskning, Kjeller, Norway.
[5]University of Leeds, Leeds, UK.
[6]Meteorological Institute, Free University of Berlin, Berlin, Germany.
[7]Naval Research Laboratory, Washington, D.C., USA.
[8]Computational Physics, Inc., Springfield, Virginia, USA.
[9]Institute of Environmental Physics, University of Bremen, Bremen, Germany.
[10]Program in Atmospheric and Oceanic Science, University of Colorado, Boulder, Colorado, USA.
[11]Cooperative Institute for Research in Environmental Sciences (CIRES), University of Colorado, Boulder, Colorado, USA.
[12]National Oceanic and Atmospheric Administration, Boulder, Colorado, USA.
[13]NASA Ames Research Center, Moffett Field, California, USA.
[14]Division of Geological and Planetary Sciences, California Institute of Technology, Pasadena, California, USA.
[15]Koninklijk Nederlands Meteorologisch Instituut, De Bilt, Netherlands.
[16]Deutscher Wetterdienst, Observatory Hohenpeißenberg, Hohenpeißenberg, Germany.
[17]Atmospheric Environment Service, Downsview, Ontario, Canada.
[18]Department of Physics, University of Wales, Aberystwyth, Wales, UK.
[19]Royal Meteorological Institute of Belgium, Brussels, Belgium.
[20]Meteorologisches Observatorium, Lindenberg, Germany.
[21]Central Aerological Observatory, Dolgoprudny, Moscow Region, Russia.
[22]Solar-Terrestrial Environment Laboratory, Nagoya University, Toyokawa, Aichi, Japan.
[23]Now at Research Center for Advanced Science and Technology, University of Tokyo, Tokyo, Japan.
[24]Sodankylä Meteorological Observatory, Sodankylä, Finland.
[25]Centre of Aerology, Legionowo, Poland.
[26]Danish Meteorological Institute, Copenhagen, Denmark.
[27]UK Met Office, Bracknell, Berkshire, UK.
[28]Valentia Observatory, Irish Meteorological Service, Cahirciveen, County Kerry, Ireland.
[29]Meteorological Research Institute, Tsukuba, Ibaraki, Japan.
[30]National Institute for Environmental Studies, Tsukuba, Ibaraki, Japan.
[31]Instituto Nacional de Técnica Aeroespacial, Torrejon de Argoz, Madrid, Spain.
[32]Fisbat Institute, Consiglio Nazionale delle Ricerche, Bologna, Italy.
[33]Czech Hydrometical Institute, Prague, Czech Republic.
[34]Swiss Meteorological Institute, Les Invuardes, Switzerland.

Copyright 2002 by the American Geophysical Union.
0148-0227/02/2001JD000533

absence of any chemical loss. The chemical loss of ozone throughout the winter was nearly balanced by dynamical resupply of ozone to the vortex, resulting in a relatively constant value of total ozone of 340 ± 50 DU between early January and late March. This observation of nearly constant total ozone in the Arctic vortex is in contrast to the increase of total column ozone between January and March that is observed during most years. *INDEX TERMS:* 0341 Atmospheric Composition and Structure: Middle atmosphere—constituent transport and chemistry (3334); 1610 Global Change: Atmosphere (0315, 0325); 9315 Information Related to Geographic Region: Arctic region; 0322 Atmospheric Composition and Structure: Constituent sources and sinks; 0340 Atmospheric Composition and Structure: Middle atmosphere—composition and chemistry; *KEYWORDS:* ozone, stratosphere, Match

Citation: Rex, M., et al., Chemical depletion of Arctic ozone in winter 1999/2000, *J. Geophys. Res.*, *107*(D20), 8276, doi:10.1029/2001JD000533, 2002.

1. Introduction

[2] In autumn and early winter, stratospheric air at high northern latitudes cools and descends, and a westerly wind circulation (the Arctic vortex) develops. If the temperature within the vortex drops below a critical level, polar stratospheric clouds (PSCs) can form [e.g., *Solomon*, 1999, and references therein]. Reactions on the surface of these clouds convert stratospheric chlorine, that is supplied primarily by the breakdown of man-made chlorofluorocarbons, from benign forms into active forms and in the presence of sunlight chlorine monoxide (ClO) destroys ozone [e.g., *Solomon*, 1999]. The strength and temperature of the Arctic vortex varies considerably from winter to winter. Unlike the Antarctic vortex which is strong and cold every winter, resulting in the so-called Antarctic "ozone hole," the Arctic winter vortex varies considerably from year to year. Since the mean Arctic vortex temperatures are near the threshold for PSC occurrence, substantial differences in the degree of chemical loss of Arctic ozone for individual winters have been observed during the past decade [e.g., *Proffitt et al.*, 1990; *Schoeberl et al.*, 1990; *Hofmann and Deshler*, 1991; *Salawitch et al.*, 1993; *Manney et al.*, 1994; *von der Gathen et al.*, 1995; *Müller et al.*, 1997; *Rex et al.*, 1997, 1999]. Accurate quantification of the chemical and dynamical influences is required for a full understanding of the effects of human activity on Arctic ozone. A number of model studies that used either measured or calculated concentrations of ClO and observed rates for the important reactions have been unable to fully account for the observed chemical loss of Arctic ozone in a quantitative manner, particularly for winters with rapid chemical loss [e.g., *Hansen et al.*, 1997; *Becker et al.*, 1998, 2000]. Given the large sensitivity of Arctic ozone to temperature and the fact that the Arctic vortex is likely to cool due to rising concentrations of greenhouse gases, it is possible that there will be an increased frequency of winters where conditions are conducive for large amounts of chemical ozone loss [*Austin et al.*, 1992; *Shindell et al.*, 1998].

[3] During the winter of 1999/2000 the EU Third European Stratospheric Experiment on Ozone (THESEO 2000) and the NASA SAGE III Ozone Loss and Validation Experiment (SOLVE) were mounted as a collaborative field campaign to better quantify the chemical and dynamical factors that regulate Arctic ozone and thereby improve our predictive capability for future changes to Arctic ozone. Measurements of ozone, numerous other atmospheric gases, and the chemical and optical properties of PSCs were made using instruments on aircraft, balloons, ground-based stations and satellites. These concerted observations resulted in the most comprehensive set of measurements ever obtained in the Arctic winter stratosphere. The work described here resulted from these experiments. The total column abundance of ozone in the Arctic vortex stayed relatively constant during the winter, with values around 330 ± 38 Dobson units (DU) during January, 350 ± 48 DU during February and 332 ± 33 DU during March 2000 (1 Dobson unit equals 10^{-3} cm thickness of gas compressed to surface pressure and temperature). These values are based on a large number of ozonesonde observations inside the Arctic vortex (Figure 1). The chemical loss of ozone in the vortex is not straightforward to quantify from observations of ozone because the abundance of ozone is also strongly affected by atmospheric dynamics [e.g., *Rex et al.*, 2000]. For winters with little or no PSC activity, the column abundance of Arctic O_3 normally increases substantially (~100 DU) due to poleward, downward transport of ozone. The wintertime ozone build up is quite variable from year to year, depending on the meteorological situation [*Chipperfield and Jones*, 1999].

[4] In this paper, we use three techniques to quantify the chemical loss of ozone that occurred during the winter of 1999/2000. The "Match" technique [*von der Gathen et al.*, 1995; *Rex et al.*, 1997, 1999] relies on calculations of air parcel trajectories to isolate changes in ozone for many individual air parcels sampled at various times and places by a large number of coordinated ozonesonde soundings. The "tracer" technique [*Proffitt et al.*, 1990; *Müller et al.*, 1997] uses the temporal evolution of correlations of the volume mixing ratio (vmr) of ozone and a long-lived gas, such as nitrous oxide (N_2O) or methane (CH_4), that serves as a tracer of dynamical motions. The "vortex-averaged" technique [*Bevilacqua et al.*, 1997; *Knudsen et al.*, 1998] involves analysis of the temporal evolution of the mean profile of ozone within the vortex along surfaces of potential temperature that descend according to rates calculated by a radiative transfer model. These are considered in turn after a brief description of stratospheric conditions in the 1999/2000 winter.

2. Presence of PSCs in Winter 1999/2000

[5] The Arctic winter of 1999/2000 was exceptionally cold. Figure 2a shows a time series of the area of the vortex cold enough for PSCs to exist, denoted A_{PSC}, at a potential temperature (Θ) level of 475 K (~19 km altitude). A_{PSC} is

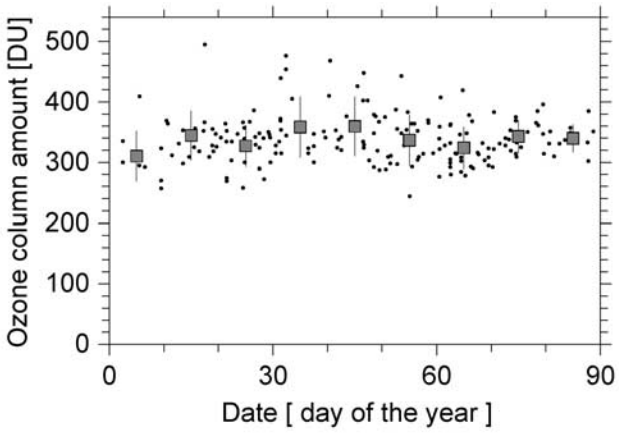

Figure 1. Evolution of the total ozone column inside of the Arctic vortex from January to March 2000 based on ozonesonde measurements. The ozone column between the surface and the termination altitude of the sounding was calculated from the measured ozone density, air pressure, and temperature profiles. The column above the termination altitude of the sounding was estimated assuming a constant ozone mixing ratio profile above. The total column was only derived from soundings that reached at least 25 km altitude. For all measurements included in the plot the estimated amount of ozone in the partial column of air above the measured profile contributes less than 15% to the total column. Due to the requirement that a minimum altitude of 25 km had to be reached by the sounding, the number of soundings included here is substantially smaller than the total number of sondes launched into the Arctic vortex during the SOLVE/THESEO 2000 campaign. Dots show the individual measurements and squares and error bars denote 10-day averages and the 1σ standard deviation.

calculated using temperatures from the European Centre for Medium-Range Weather Forecasts (ECMWF) and an assumption of thermodynamic equilibrium with nitric acid trihydrate (NAT), the most stable phase of PSCs that occur at temperatures above the water frost point [*Hanson and Mauersberger*, 1988]. Figure 2b shows the vertical distribution of A_{PSC} through December 1999 to March 2000. Significant areas with PSC-conditions first occurred around mid-December, covering a vertical region between potential temperatures of ~450–600 K. This first period of low temperatures lasted until early February. During that time the vertical extent of significant A_{PSC} moved to lower altitudes and covered the region between ~400 and 500 K at the beginning of February. A minor warming occurred during February and A_{PSC} dropped to low values around mid-February. A second cold spell started in the last days of February and lasted to about mid-March. During this period significant values of A_{PSC} were limited to the region below ~450 K. Also shown in Figure 2b are observations of the location of PSCs obtained during the 1999/2000 winter season by the Polar Ozone Aerosol and Monitoring (POAM III) satellite instrument [*Lucke et al.*, 1999; *Hoppel et al.*, 2002] and by a ground-based lidar [*Beyerle et al.*, 1994]. These comparisons indicate that A_{PSC} provides a reasonable estimate of the height and times for which PSCs were actually observed. For much of the 1999/2000 winter, the area of PSCs in the Arctic vortex at Θ = 475 K exceeded area estimates for the equivalent dates during any previous winter of the past two decades.

3. Chemical Ozone Loss Based on Match

[6] A Match campaign [*Rex et al.*, 1997, 1998, 1999], consisting of measurements of ozone from a total of 770 ozonesondes launched from 29 stations, was carried out to quantify the chemical loss of ozone during the winter of 1999/2000. The ozonesonde launches were coordinated in real time to probe several hundreds of air masses twice over a several-day interval (so-called "match events"). The coordination was based on calculations of air parcel trajectories (using wind fields from ECMWF) that allow for diabatic descent. The descent rates are calculated using the radiative transfer scheme of the SLIMCAT 3-D chemical transport model [*Chipperfield*, 1999], which uses UKMO analyses for stratospheric winds and temperatures and the ozone field that was calculated by SLIMCAT. Chemical loss rates are derived from a statistical analysis of many match events by subtracting the first measurement of ozone from the second. Further details of the Match technique, including a discussion of quality checks on the match events and on the ozonesonde data, are provided by *Rex et al.* [1999]. The quality checks as described by *Rex et al.* [1999] were applied unchanged, with the exception that the maximum "match radius" [cf. *Rex et al.*, 1999] was set to 400 km instead of 500 km. In winter 1999/2000 this reduction in the maximum match radius resulted in a reduced statistical uncertainty of the results. All results presented here are based on Match events that took place inside the Arctic polar vortex. We have chosen a value of 36 s^{-1} normalized potential vorticity to define the edge of the vortex [see *Rex et al.*, 1999]. This value is close to the maximum horizontal gradient in normalized PV, that varied between values of 35 and 40 s^{-1} between early January and late March. Due to the steep PV gradient at the edge of the vortex, the area enclosed by the narrow PV interval between 36 s^{-1} and the maximum horizontal gradient in PV is negligible and no Match events occurred in this area; that is, for Match, both definitions of the vortex edge are equivalent.

[7] Chemical ozone loss rates from Match are shown on three potential temperature surfaces in Figure 3. The loss rates are expressed in two ways: as ozone loss per sunlit time (Figures 3a, 3c, and 3e; see *Rex et al.* [1999] for the definition of the sunlit time) and as ozone loss per day (Figures 3b, 3d, and 3f). The evolution of A_{PSC} on the respective potential temperature surface is indicated in the upper part of each panel. The ozone loss per sunlit time reached a peak value of about 6 ppbv (parts per billion volume) per sunlit hour on the 500 and 550 K surfaces in late January. Due to the increasing sunlight in Arctic spring, the ozone loss per day peaked in early March, with rates of up to 61.6 ± 4.8 ppbv per day on the 450 K surface. All errors stated in this paper denote the 1σ uncertainty.

[8] The vertical distributions of the ozone loss rates from Match in the range from Θ = 400 to Θ = 575 K are given in Figures 4b (ppbv per sunlit hour) and 4c (ppbv per day). To allow a better comparison with Figure 2, the 4.10^6 km^2 isoline of A_{PSC} is also shown in these panels. A first period

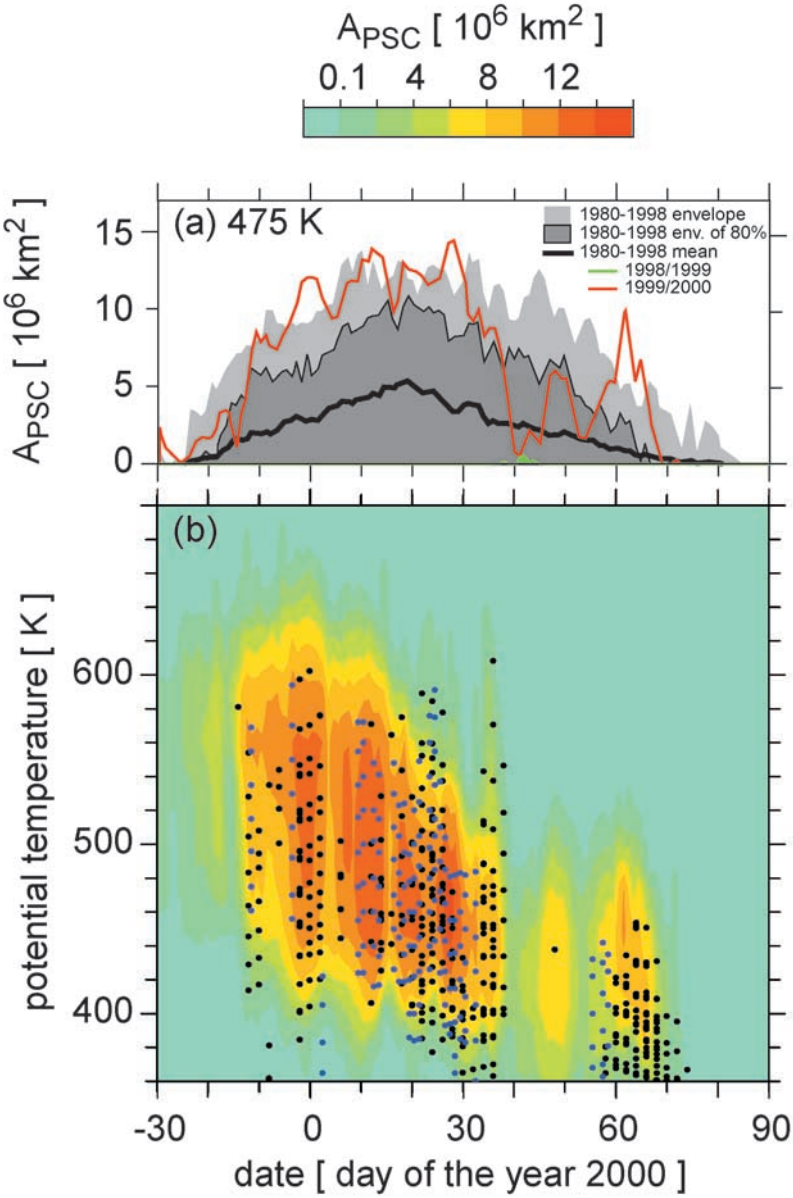

Figure 2. (a) The area of the Arctic at Θ = 475 K potentially populated by PSCs, A_{PSC}, based on temperatures from ECMWF and the thermodynamics of nitric acid trihydrate from *Hanson and Mauersberger* [1988] (see *Rex et al.* [1999] for details). Curves of A_{PSC} for winters of 1999/2000 (red) and 1998/1999 (green line near day 40) are shown. The mean, variance (envelope of 80% the data), and extreme of A_{PSC} for all winters between 1980/1981 and 1997/1998 are also shown. (b) Vertical distribution of A_{PSC} (values indicated on colorscale). The height of PSC appearance observed by POAM III on specific days between 63 and 68 N (black dots) and by a ground-based lidar at Ny Ålesund (79 N, 12 E) (blue dots). The lidar operated about 65% of the days due to weather, with significant gaps (longer than a couple of days) only during late December/early January, when about one observation per week was obtained.

of ozone loss occurred from mid-January to early February and had a vertical extent from Θ = 460 to 570 K, with the highest rates between 480 and 540 K. The ER-2 observations during the late January and early February 2001 were generally obtained at and below potential temperature levels of 430–465 K; therefore the finding of *Richard et al.* [2001] of insignificant chemical loss of ozone during this period is, within the error bars, consistent with the Match results shown in Figure 4b. A second period of rapid loss was observed from late February to late March. During this time the loss was limited to the region below 520 K. Figures 3 and 4 show that the vertical distribution and the time evolution of rapid ozone loss correlates well with the vertical distribution and evolution of A_{PSC}.

[9] Figure 4a shows the evolution of the vortex-averaged peak vmr of ClO observed by the Airborne Submillimeter

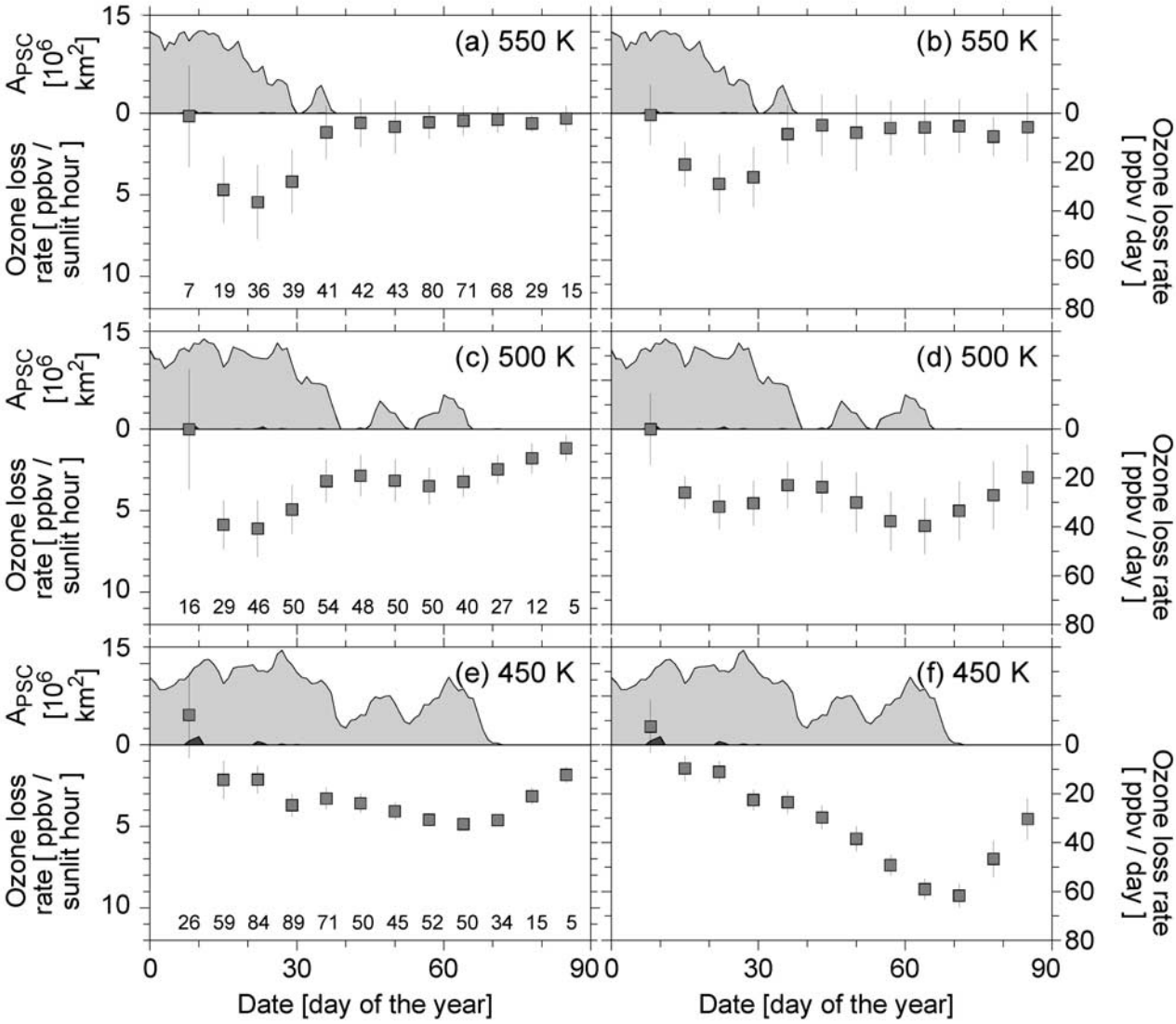

Figure 3. (a and b) Ozone loss rates from Match (squares) at Θ = 550, (c and d) 500 and (e and f) 450 K in ppbv per sunlit time (Figures 3a, 3c, and 3e), and ppbv per day (Figures 3b, 3d, and 3f). The loss rates represent the results of linear regressions over match events in ±10 day broad bins. The numbers at the lower part of Figures 3a, 3c, and 3e give the number of individual match events used in the respective linear regression. A_{PSC} is also indicated for each potential temperature surface as the shaded area in the upper part of the respective panels.

Radiometer (ASUR) [*Bremer et al.*, 2002, and references therein] on the DC-8 research aircraft. The absolute value of the peak vmr plotted in Figure 4a is influenced by the instrumental resolution (∼6–10 km in the lower stratosphere; this corresponds approximately to 120–200 K in Θ coordinates). However, the relative change in the abundance of ClO is well represented by the ASUR measurements. Due to the vertical resolution of ASUR, the measurements of ClO shown in Figure 4a represent basically the average ClO vmr over the vertical region shown in Figure 4b. The vertically integrated loss of ozone in the partial column between 400 and 575 K is shown in Figure 4d (DU per sunlit hour) and Figure 4e (DU per day). Vortex-averaged profiles of pressure and temperature at the respective date, based on all ozone soundings inside the vortex within ±5 days around that date, were used to compute column loss from the profile of loss rates, given in vmr versus Θ. The ozone column loss per sunlit time reached a maximum in late January and then generally declined until late March, in concert with the evolution of ClO, which showed larger concentrations in late January and declined by a factor of 2–3 by mid-March. However, due to increasing sunlit time per day, the column loss per day peaked at 2.4 ± 0.3 DU per day during early March. The minimum of both loss rates in mid-February coincides with a warming of the vortex that is evident from the minimum for A_{PSC} during that time.

[10] The altitude of the maximum ClO vmr derived from the ASUR measurements (black bars in Figure 4b) was at ∼500 K in January and ∼450 K in March, which coincides with the respective altitudes of the maximum ozone loss

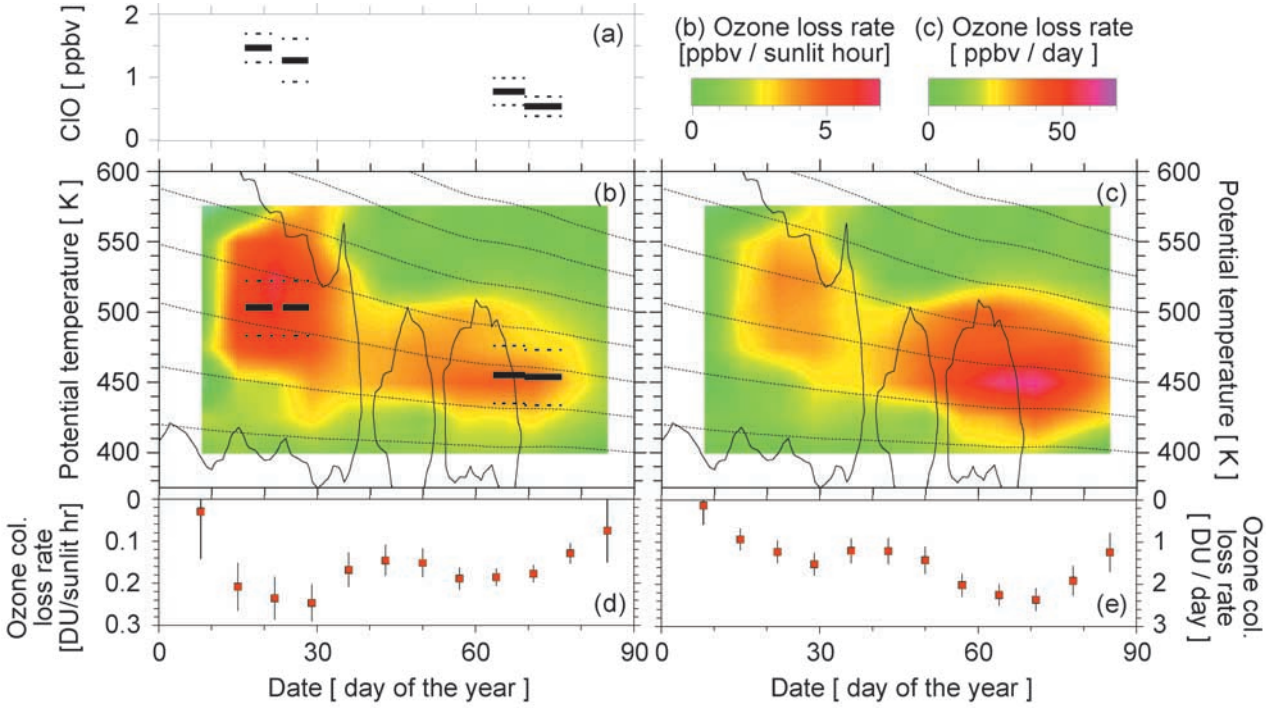

Figure 4. (a) The vortex-averaged peak vmr of ClO from ASUR. The data obtained by ASUR on several flights has been averaged into 5–7 day bins. Only measurements inside the polar vortex at solar zenith angles less than 87° have been used. Vertical distribution of the ozone loss (b) per sunlit time and (c) per day. The black contours show the 4.10^6 km^2 isoline of A_{PSC} (cf. Figure 2b). The black dotted lines show the subsidence of air masses as derived from SLIMCAT (see section 5 and *Rex et al.* [1999] for details). The altitudes of the peaks in the ClO profiles from ASUR are also shown (black bars in Figure 4b; the corresponding dotted lines represent the estimated uncertainties of the retrieval, under the assumption of a sufficiently symmetric ClO profile). Vertically integrated chemical ozone loss rate in the column of air between Θ = 400 and 575 K in loss (d) per sunlit hour and (e) per day.

rates during these periods. Figure 5 compares the vertical distribution of the ozone loss rate derived from Match for early March with a profile of the ClO mixing ratio measured in situ inside the vortex on 1 March by an resonance fluorescence balloon-borne instrument (HALOZ) [*Vömel et al.*, 2001].

[11] The vertical region of fast ozone loss coincides reasonably well with the region of high concentrations of ClO observed by HALOZ, given that the ozone loss rates are vortex averages and the measurements of ClO represent conditions at one particular location in the Arctic vortex. This observation is consistent with observations from previous winters [*Pierson et al.*, 1999; *Woyke et al.*, 1999] and strongly supports the notion that the ozone loss in the Arctic is caused by elevated concentrations of active chlorine. A more quantitative analysis of the relation of chemical loss of ozone and the ClO vmr as measured by HALOZ is given by *Vömel et al.* [2001].

[12] We now turn to the accumulated chemical losses of ozone in particular layers of air within the Arctic vortex. In the vortex during winter, diabatic cooling results in subsidence and the potential temperature of air parcels is not conserved. The subsidence of air parcels must be accounted for in the calculation of integrated chemical loss of ozone. We do this by examining the change in ozone along surfaces of "adjusted potential temperature" ("aΘ"), where aΘ is defined as the potential temperature a parcel would achieve on 31 March using vortex average descent rates. As above, descent rates are calculated using the radiative transfer scheme of the SLIMCAT model. For the period and vertical extent considered, diabatic subsidence derived from inert tracer observations obtained during SOLVE/THESEO 2000 agrees to better than Θ = 10 K with the calculated subsidence [*Greenblatt et al.*, 2002b].

[13] The time evolution of the vortex-averaged accumulated ozone loss in subsiding layers is given in Figure 6a. During January to mid-March, when sufficient POAM III ozone measurements inside the polar vortex are available, the evolution, the vertical structure and the degree of chemical ozone loss shown in Figure 6a are in good quantitative agreement (better 20% throughout) with the accumulated ozone losses derived from POAM data [*Hoppel et al.*, 2002, Figure 5]. The accumulated loss from 9 January (day 8) through 26 March (day 85) is plotted versus a$\Theta\Theta$ in Figure 6b. It peaks at 2.7 ± 0.24 ppmv (parts per million volume) for air at Θ = 453 K on 26 March. This is the largest local chemical ozone loss ever observed during Arctic winter. This result agrees well with results from *Sinnhuber et al.* [2000], who reported chemical ozone loss of 2.5 ppmv at 450 K for one particular station inside the Arctic vortex, and shows that this large loss of ozone was representative of the whole vortex. It is

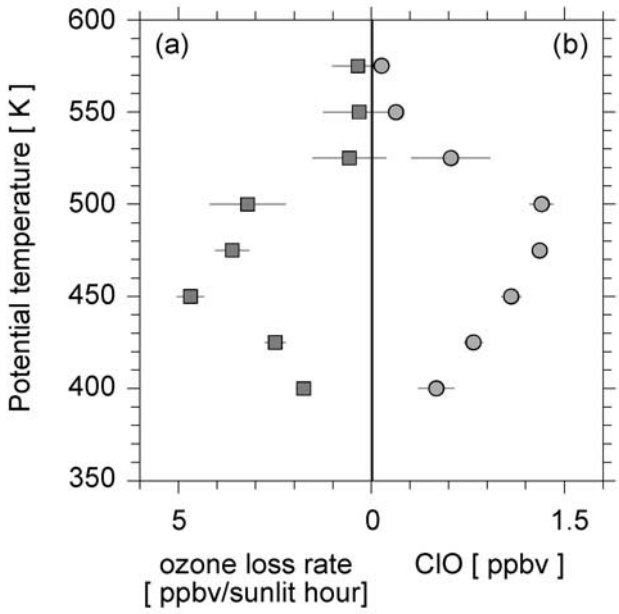

Figure 5. (a) Vertical profile of ozone loss rates on 1 March 2000 (±10 days) from Match. (b) The ClO profile measured by HALOZ on 1 March 2000 close to local noon. For better comparison with the Match data, the original data has been averaged into 25 K bins. The error bars are based on the scatter of the individual data points.

also generally consistent with reports of significant ozone decreases inside the polar vortex by *Santee et al.* [2000]; however a quantitative comparison with that study is not possible because the effect of diabatic subsidence on ozone change was not taken into account by *Santee et al.* [2000].

[14] In the previous paragraphs the results from Match have been regarded as average values over the Arctic vortex. We now analyze how well different parts of the vortex are represented by the Match results. Figure 7 shows the distribution of match events in potential vorticity space for the three isentropic surfaces shown in Figure 3 (low values of relative PV correspond to the inner most region of the vortex; see caption). Throughout most of the observing time the vortex was fully covered by match events, with a generally slight under representation of the outer part of the vortex. This is particularly true during March at the lower potential temperature levels, where the outer 50% of the vortex area was not sampled.

[15] Figure 8 shows the ozone loss rates in different parts of the polar vortex for two different periods, i.e., January/early February (squares) and late February/March (crosses). Generally the ozone loss rate at the edge of the vortex tended to be smaller than the vortex average. Otherwise the ozone loss was relatively homogenous within the polar vortex. During March no results could be obtained for the outer 50% of the vortex at $\Theta = 450$ K because this area was not sufficiently sampled by match events (cf. Figure 7)

[16] Based on theoretical considerations [e.g., *Solomon*, 1999, and references therein] and experimental results [*Rex et al.*, 1999] we know that Arctic ozone loss occurs exclusively in sunlit air masses. Therefore any oversampling or undersampling of the southern and more sunlit parts of the vortex or the darker northern regions may lead to differences between the ozone loss inferred from the Match observations and the true vortex average. Since low PV areas do not always correspond to the southernmost and most sunlit parts of the vortex, it may not be sufficient to look at the sampling of the vortex in PV space to assess the representativeness of the results. Figure 9 compares the vortex-averaged sunlit time per day with the same quantity along the trajectories used in the Match analysis. The exposure to sunlight along the Match trajectories generally reflects average conditions throughout the vortex very well. Only in January, particularly at the higher potential temperature levels, the average exposure to sunlight of the air parcels sampled by Match is slightly less than for the vortex

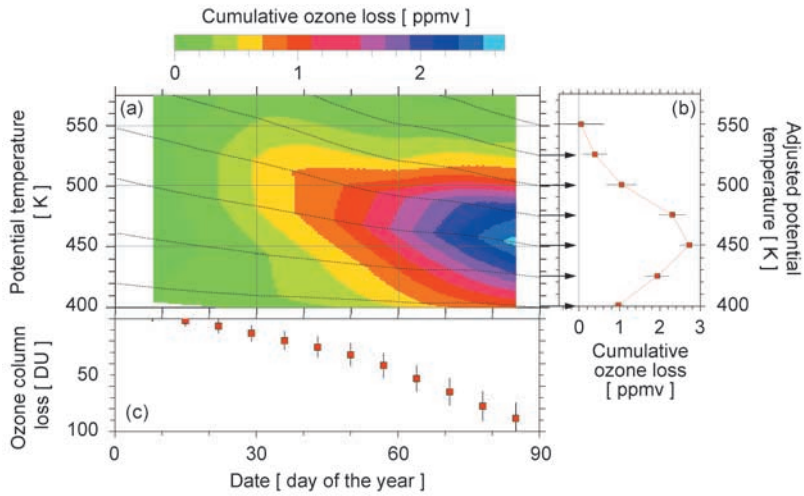

Figure 6. (a) Evolution of the accumulated ozone loss in subsiding air masses from Match. (b) Profile of the accumulated ozone loss on 26 March 2000 (day 85) from Match. (c) Accumulated chemical ozone loss in the partial column between $\Theta = 400$ and 575 K from Match (column $[O_3^*\text{-}O_3]$; see section 6 for details).

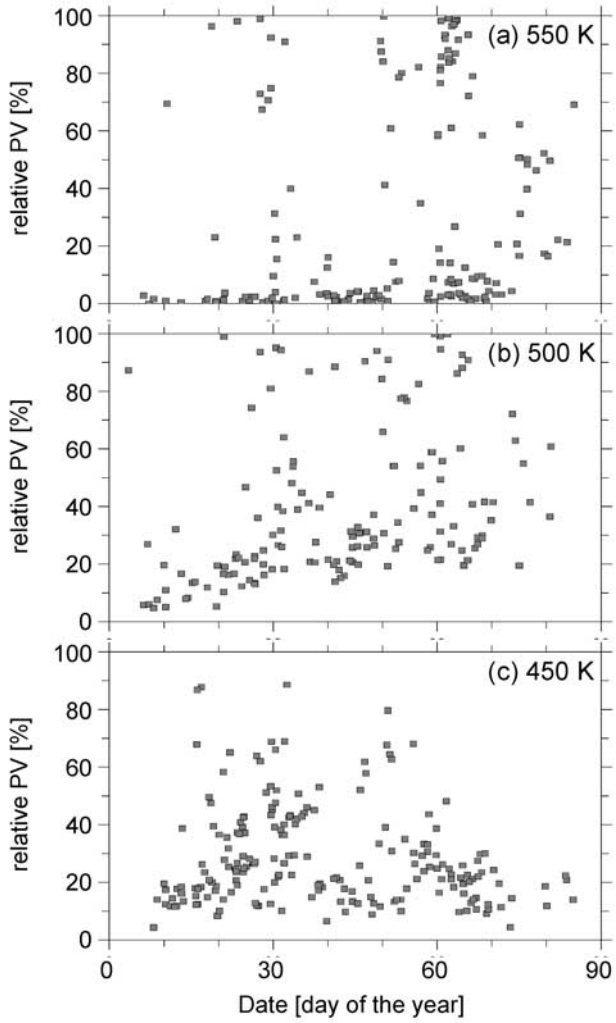

Figure 7. Sampling of the polar vortex with Match events at (a) $\Theta = 550$, (b) 500, and (c) 450 K. The PV value of each match event is plotted against date. To elucidate the homogeneity of the sampling, the PV values of the matches are mapped on a relative PV scale, which runs from 0 for the maximum PV value reached at the center of the vortex on a given day, to 1 at the vortex edge. The relation between PV and relative PV is chosen such that, for each day, equal intervals in the relative PV scale correspond to equal fractional areas of the polar vortex, i.e., a relative PV of 40% means that 0.4 of the vortex area is enclosed by the corresponding isoline of PV.

average and is more comparable to conditions for the inner 50% of the vortex area. Based on the data shown in Figure 7 and the comparisons shown in Figure 9, it is valid to consider the ozone loss rates from Match to be generally representative of the vortex average ozone loss.

4. Chemical Ozone Loss Based on Tracer Relations

[17] The change in the relation between mixing ratios of O_3 and long-lived tracers such as N_2O and CH_4 can also be used to quantify chemical loss of ozone [*Proffitt et al.*, 1990; *Müller et al.*, 1997]. Figure 10 shows the evolution of the O_3 versus N_2O relation observed by three flights in the Arctic vortex by the NASA Observations of the Middle Stratosphere (OMS) balloon-borne in situ and remote instrument payloads and for a few selected flights of the NASA ER-2 aircraft. Comprehensive discussions of chemical ozone loss rates based on the ER-2 observations is provided by *Richard et al.* [2001] and on the OMS observations by *Salawitch et al.* [2002]. Our focus is on chemical loss from the balloon observations and the use of the ER-2 observations to demonstrate that, for the winter of 1999/2000, transport of air across the edge of the vortex could not have been responsible for the dramatic change observed in the O_3 versus N_2O relation. A description of the OMS balloon-borne instruments and measurement sensitivities for observations used in our analysis is provided by *Salawitch et al.* [2002]. A similar description of ER-2 instruments and sensitivities is provided by *Richard et al.* [2001].

[18] Isolated descent of purely vortex air will preserve the initial O_3 versus N_2O relation [*Proffitt et al.*, 1990]. Neglecting for now any possible effects of transport on the O_3 versus N_2O relation, the reduction in the mixing ratio of O_3 during the course of the winter, for constant values of N_2O, signifies chemical loss of O_3. The largest source of uncertainty in the estimate of chemical loss from the tracer observations is the initial abundance of O_3 prior to chemical loss. Only two individual profiles are available to establish this initial relation, which differ by about ~20% in the relevant vertical region, probably due to true atmospheric variability [*Salawitch et al.*, 2002] The excellent agreement between the O_3 versus N_2O relation measured by the OMS in situ package on 5 March 2000 and by the ER-2 on this same date, for different geographic regions deep inside the vortex, demonstrates that this profile is representative of conditions in a broad region deep inside the vortex on this day. The balloon-borne observations shown in Figure 10 indicate that chemical reactions inside the vortex led to removal of 1.0 to 1.5 ppmv of O_3 for air sampled between $\Theta = 430$ and 460 K (~17–19 km) on 5 March 2000. This compares well with Match estimates for chemical loss of 1.1 ± 0.3 ppmv at $\Theta = 430$ K and 1.7 ± 0.3 ppmv at $\Theta = 460$ K for the same date. *Richard et al.* [2001] show, based on analysis of ER-2 data, that the accumulated chemical ozone loss reached $58 \pm 4\%$ near 450 K by 12 March 2000, which is also in good agreement with estimates from Match for that time and altitude.

[19] The validity of the chemical loss of ozone estimated in this manner is dependent on whether transport of air, particularly mixing across the vortex edge, changes the O_3 versus N_2O relation. *Michelsen et al.* [1998] and *Plumb et al.* [2000] have suggested that before chemical loss of ozone occurred, mixing between subsided inner vortex air with extravortex air may lead to a flattening out of the curved O_3/N_2O relation and thus may be mistaken as chemical loss of ozone. However, the effect of mixing on this relation largely depends on the shapes of the inner vortex and extravortex relations between O_3, N_2O and Θ throughout the winter. Observations of O_3 versus N_2O obtained by ER-2 instruments in the core of the vortex on 23 January (orange dots, Figure 10) and on 7 March (green dots, Figure 10) show evidence for some entrain-

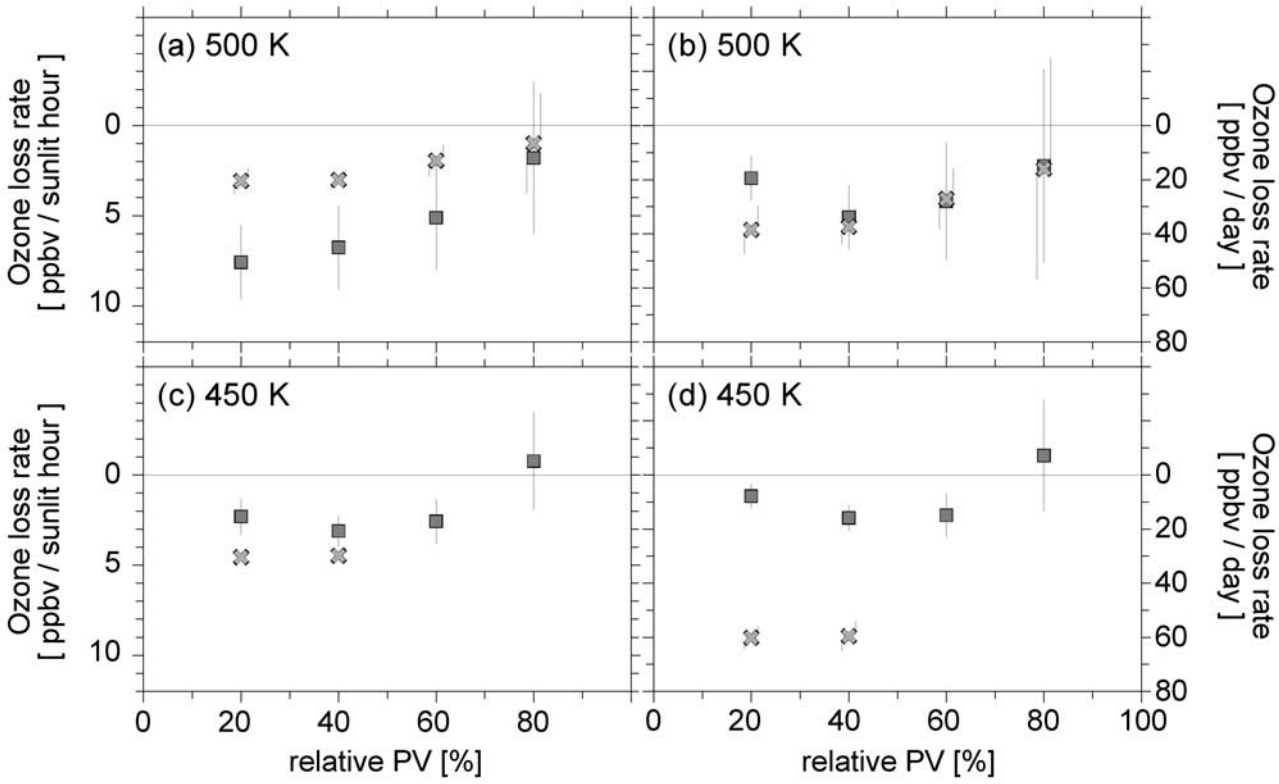

Figure 8. Ozone loss rates in different parts of the vortex for (a and b) Θ = 500 and (c and d) Θ = 450 K for the period 10 January to 5 February (red squares) and 25 February to 25 March (green crosses). Figures 8a and 8c show the ozone loss per sunlit hour, Figures 8b and 8d show the daily ozone loss. The ozone loss rates are plotted against relative PV (cf. caption of Figure 7).

ment of extravortex air into the core of the vortex during the winter, which allows us to assess the effect that such mixing had on the O_3/N_2O relation. The darker colored points in Figure 10 indicate measurements obtained in relatively narrow filaments of air along surfaces of near constant potential temperature (Θ = 462 ± 5 K for 23 January and Θ = 453 ± 3 K for 7 March). These observations indicate various degrees of mixing between air parcels originating from inside the vortex (O_3 versus N_2O close to the unmixed, vortex relation) and air originating outside the vortex (higher values of O_3 and N_2O). The measurements convincingly demonstrate that entrainment of extravortex air led to an increase in the mixing ratio of O_3 for a given value of N_2O, given the prevailing inner vortex and extravortex relations between O_3, N_2O, and Θ for January and March 2000. Although in section 6 we show that entrainment of extravortex air did not significantly alter the composition of the vortex (strong mixing lines inside the vortex were relative scarce during all the ER-2 flights; see *Greenblatt et al.* [2002a] for a statistic of mixing events during the ER-2 flights), whatever entrainment did occur during the time of chemical loss for this winter increased O_3 at a given level of N_2O inside the vortex. Thus the overall changes in the O_3 versus N_2O relation observed during the course of winter could not have been caused by transport, and rather represent a lower limit for the true chemical loss of ozone. Further demonstration that transport alone could not have led to the observed changes in the O_3 versus N_2O relation for the winter of 1999/2000 is provided by *Richard et al.* [2001], *Ray et al.* [2002], and *Salawitch et al.* [2002].

5. Chemical Ozone Loss Based on Vortex Average

[20] Changes in the vortex-averaged ozone vmr profile in aΘ coordinates can only be caused by either chemical loss or by transport of ozone across the edge of the vortex. Figure 11a shows the evolution of vortex-averaged ozone profiles in aΘ coordinates. To minimize the effects of transport, we used the maximum gradient of PV to define the vortex edge. Comparison of the black solid line (ozone in early January versus aΘ) to the dotted line (ozone in early January versus Θ) in Figure 11a illustrates the degree of subsidence computed by the SLIMCAT model. The accumulated chemical loss of ozone (the difference between the black solid and red solid lines) peaks at 2.6 ppmv for the aΘ = 460 K level.

[21] A critical test of chemical ozone loss based on the "vortex-averaged" technique is given in Figure 11b. The largest uncertainty of the vortex average approach is introduced by possible exchange of air across the vortex edge. In Match, synopticscale intrusions of extravortex air are explicitly accounted for and great care is taken to

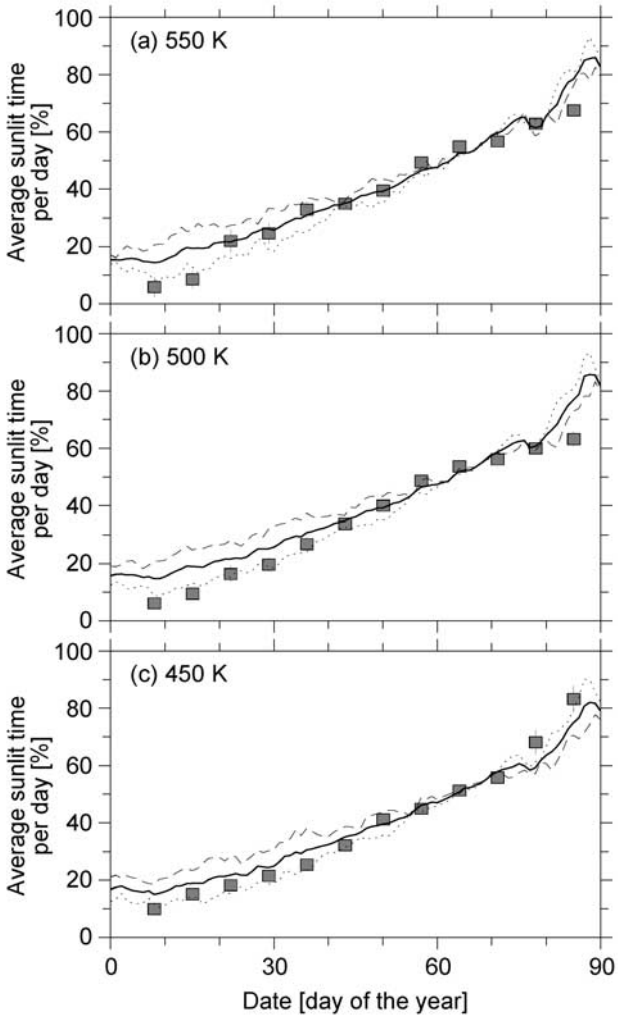

Figure 9. Comparison of the average sunlit time per day along the trajectories that have been used for the Match analysis (squares) with vortex average conditions (solid line) at (a) Θ = 550, (b) 500, and (c) 450 K. The dotted and the dashed lines show the average sunlit time per day in the inner 50% area of the vortex (based on PV analyses) and the outer 50% area, respectively.

avoid areas of potential smallscale mixing [see *Rex et al.*, 1999]. A comparison between accumulated ozone loss from the Match analysis and from the vortexaveraged approach allows us to assess the potential influence of entrainment of extravortex air on the vortexaveraged ozone profile. The red points in Figure 11b show the accumulated ozone loss between early January and late March from Match (cf. Figure 6b). Differences between the vortex average profile of O_3 versus aΘ measured in early January and profiles measured at successive times are given by the colored lines in Figure 11b. The red solid line represents the total accumulated loss of ozone between early January and late March based on vortex average ozone in aΘ coordinates. The accumulated ozone loss found using these two approaches does not show significant discrepancies, indicating that the vortex-averaged ozone was not strongly influenced by transport of air across the edge of the vortex and that the observed reductions in ozone were predominantly due to chemistry.

6. Effects of Chemistry on Ozone Column

[22] Two different quantities can be used to describe the overall chemical loss of ozone in the total column of air. First, the amount of ozone that was lost during the winter is given by the number of ozone molecules that have been destroyed during the winter in a vertical column of air inside the polar vortex. This quantity is calculated as the time integral of the column loss rate of ozone and is here denoted $\int$column $[-dO_3/dt_{chem}]$. Second, the impact of the overall chemical loss on the actual column abundance of ozone can be described by the difference between the column ozone that would have been present in the absence of chemical loss

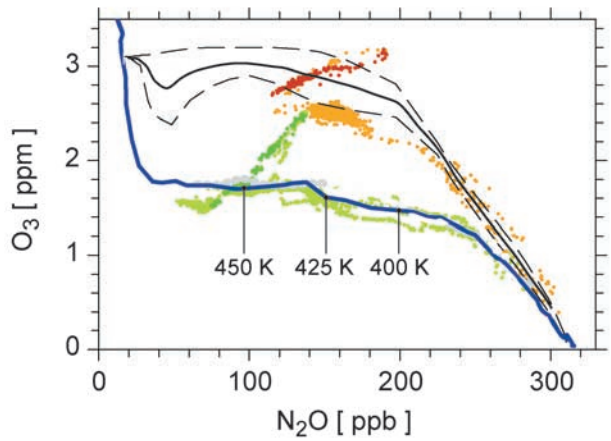

Figure 10. Measurements of the mixing ratio of O_3 versus N_2O obtained during various balloon and ER-2 flights. Measurements from the in situ (lower dashed line) and remote (upper dashed line) OMS balloon payloads on 19 November 1999 and 3 December 1999, respectively, and the average of these two relations (black solid line) are shown. Measurements from the in situ OMS balloon payload on 5 March 2000 are also shown (blue line). The balloon flights originated from a launch facility at Esrange, Sweden (68 N, 21E) and sampled the vortex based on analyses of PV [see *Salawitch et al.*, 2002]. The ER-2 measurements on 23 January 2000 (orange/red dots), 5 March 2000 (dashed gray line), and 7 March 2000 (light/dark green dots) were obtained for flights in the core of the vortex, based also on PV analyses. The ER-2 observations have been averaged onto a 10 s resolution time grid. For each time step, the average value of N_2O is computed from whichever observations are available from the ARGUS, ALIAS, and ACATS instruments. The averaging procedure places greater emphasis on data from the tunable diode laser ARGUS and ALIAS instruments, since measurements from these devices are reported at greater time resolution than are measurements from the ACATS gas chromatograph. High time resolution observations are critical for characterizing the mixing lines observed on 23 January 2000 at Θ = 462 ± 5 K and on 7 March 2000 at Θ = 452 ± 2 K, which are denoted by dark red and dark green color.

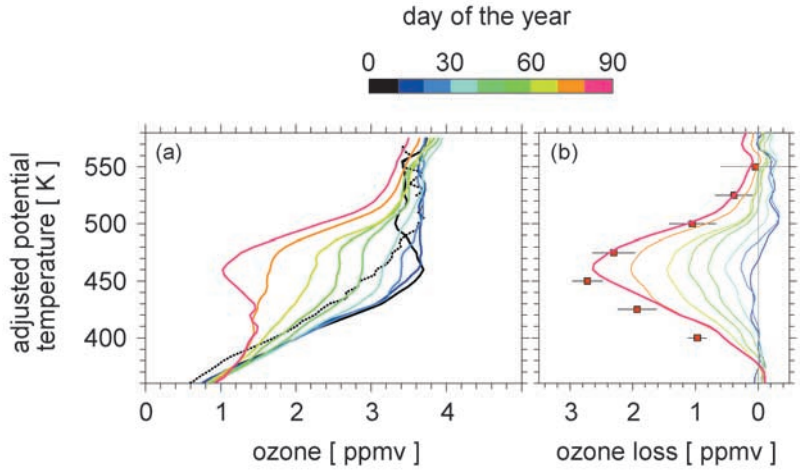

Figure 11. (a) Evolution of the average ozone profile inside the polar vortex in aΘ coordinates (see section 5). The data from all ozonesonde measurements inside the vortex have been averaged into 10 day bins, centered around the day indicated by the colorscale. The black dotted line shows the average profile for 5 January 2000 (±5 days) with Θ as the vertical coordinate (i.e., subsidence not applied). (b) Accumulated ozone loss from Match between 8 January 2000 and 26 March 2000 (red squares, cf. Figure 6b) and differences between the average profile of O_3 versus aΘ measured in early January and profiles measured at successive times (colored lines, as indicated by the scale). The last vortex-averaged ozone profile (red solid line) is for 26 March 2000, ±5 days.

(dynamics being equal), denoted column [O_3*], and the observed column abundance of ozone. We denote this second estimate of column loss as column [O_3*-O_3]. Due to subsidence and compression of air, the profile of O_3* (and hence column [O_3*]) changes with time. Several methods, as described below, are used to estimate column [O_3*].

[23] These measures of column ozone loss (e.g., $\int$column [$-dO_3/dt_{chem}$] and column [O_3*-O_3]) are different geophysical quantities. In the presence of subsidence in a non-cylindrical vortex; i.e., the presence of average poleward (or equatorward) motion, exchange of ozone depleted air masses across the surface of a cylindrical column occurs, even in the absence of exchange of air across the non-cylindrical vortex edge. The calculation of $\int$column [$-dO_3/dt_{chem}$] is insensitive to whether ozone depleted air masses later leave the cylindrical vertical column, or whether air masses that encountered ozone loss elsewhere enter this vertical column (this assumes, of course, that average conditions in the actual vortex are well sampled throughout the period of observation). However, column [O_3*-O_3], like the column amount of any chemical species, can be altered by dynamical processes. Simply put, column [O_3*-O_3] is not a dynamically conserved quantity, whereas $\int$column [$-dO_3/dt_{chem}$] is conserved. Both measures of column loss have physical meaning. The quantity $\int$column [$-dO_3/dt_{chem}$] represents the total number of ozone molecules destroyed by chemistry and is most appropriately compared to "book keeping" calculations of chemical loss, either from three-dimensional (3-D) model simulations or from model estimates constrained by measured ClO. Column [O_3*-O_3] is the true measure of the effect of chemical loss of ozone on the resulting radiative environment experienced at the ground underneath the Arctic vortex at the end of the winter and is most appropriately compared to the difference between "passive" ozone and "chemically active" ozone in 3-D model simulations.

[24] The quantity column [O_3*-O_3] is either calculated as the vertical integral of the difference between O_3 and estimates of O_3*, as derived from various approaches (see below), or as vertical integral of the accumulated ozone losses from Match (the vertical integral of the data in Figure 6b). The quantity $\int$column [$-dO_3/dt_{chem}$] is calculated by first vertically integrating the ozone column loss rates from the profiles of local ozone loss rates (data in Figure 4c) using the relation between aΘ and geometric altitude (z), as well as the density (ρ) profile at the respective time of the integration, and then accumulating these ozone column loss rates over the course of the winter (i.e., the time integral of the data in Figure 4e). Since the relation between aΘ and z, as well as the profile of ρ, are functions of time, the results of the two calculations are indeed different.

[25] Time integration of the data in Figure 4e yields $\int$column [$-dO_3/dt_{chem}$] = 117 ± 14 Dobson units (~35% of the total column present in March), similar to values of $\int$column [$-dO_3/dt_{chem}$] derived from Match experiments in previous cold Arctic winters (e.g., the winter of 1994/1995, as described by *Rex et al.* [1999]). Although chemical loss of ozone at Θ = 450 K during 1999/2000 was larger than found during any previous winter, the chemical loss extended over a broader vertical region during both 1994/1995 and 1995/1996, resulting in comparable amounts of column loss.

[26] The effect of this chemical loss on the column amount of O_3 during the Arctic winter of 1999/2000 is perhaps best visualized by comparing measured profiles of the concentration of O_3 to estimates of O_3*. Figure 12 compares profiles of O_3 measured in the Arctic vortex by different instruments (an in situ balloon photometer (Figure 12a) [*Salawitch et al.*, 2002], the POAM III satellite (Figure 12b) [*Hoppel et al.*,

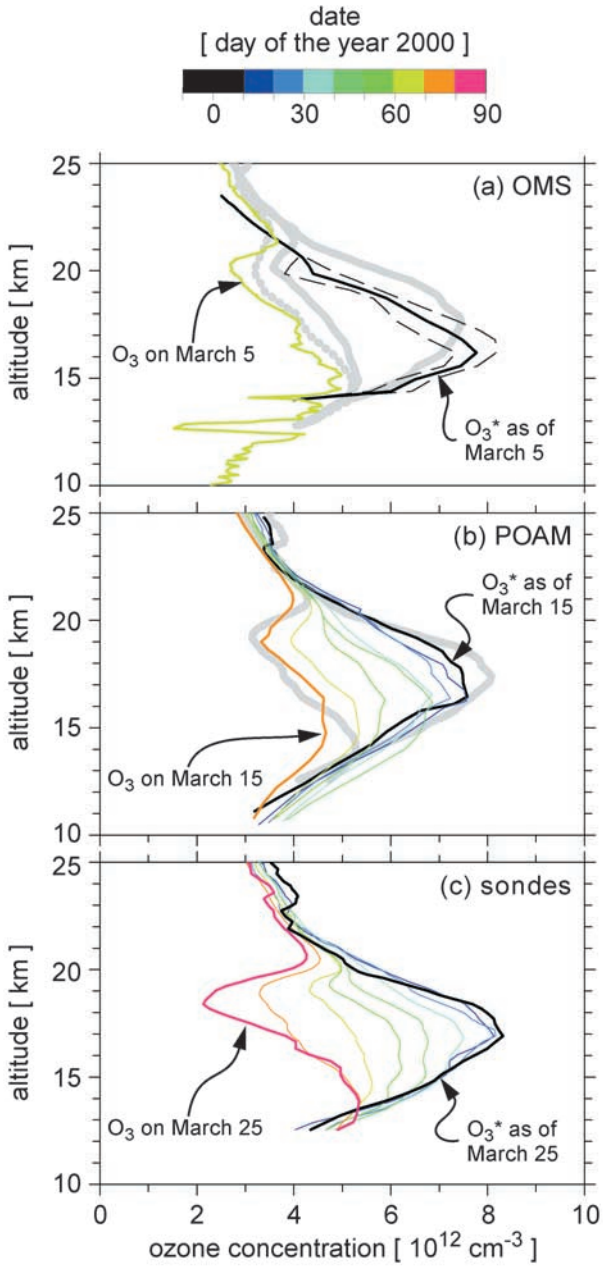

2002], and ozonesondes (Figure 12c)) to profiles of O_3* that are estimated in different ways from early winter measurements of the respective instruments. The different dates for which O_3 and O_3* are plotted in the various panels correspond to the day for which the last inner vortex O_3 profile could be determined from the respective data set. To facilitate comparisons of the sonde data with the OMS and POAM III measurements, profiles of O_3 and O_3* from the sondes for the indicated dates are shown by the solid gray lines on Figures 12a and 12b.

[27] The individual profiles for O_3 and O_3* plotted in Figure 12a reflect the local conditions in the air masses that have been sampled by the balloon instruments during the respective flights and do not necessarily represent vortex average conditions. Given this limitation, the agreement with the sonde data is reasonable. The balloon-borne observations specifically targeted the core of the vortex. Restricting the sonde profile of O_3 for 5 March to observations obtained only in the core of the vortex results in reasonably good agreement with the photometer profile. Average profiles of O_3 inside the vortex (gray dotted line, Figure 12a) were obtained by the POAM III satellite instrument until 15 March 2000 (Figure 12b) [*Hoppel et al.*, 2002]. Subsequently, the vortex was too close to the pole to be observed. Overall good agreement is found between profiles of O_3 and O_3* from POAM III for 15 March and the corresponding sonde profiles.

[28] For calculating column [O_3*-O_3] from the profiles of O_3 and O_3*, the vertical integral is evaluated between limits of 14 and 24 km. The upper limit reflects the approximate maximum altitude of PSC-initiated chemical loss. The lower limit corresponds to the Θ = 400 K surface, commonly considered to represent the bottom of the vortex circulation. Below this level, polar and extrapolar air parcels mix vigorously and it is unlikely that any of our methods for estimating chemical loss of ozone is valid.

[29] An overview over the different estimates of column [O_3*-O_3] as derived from ozone and tracer observations of the OMS balloon, the POAM III satellite measurements and the Match experiment is given in Table 1. The value of column [O_3*-O_3] derived from the tracer observations (Figure 12a) as of 5 March is 61 ± 14 DU. The largest source of error is uncertainty in the profile of O3*, which is due to observed variability in the initial O_3 versus N_2O relation (see *Salawitch et al.* [2002] for further details of this calculation). Column [O_3*-O_3] inferred from the sondes for that day is 51 DU and Column [O_3*-O_3] from Match is 53 ± 12 DU for the same day. We find column [O_3*-O_3] = 67 DU

Figure 12. (opposite) Concentration profiles of O_3 (thin colored lines) during late winter for observations from (a) the OMS balloon-borne in situ O_3 photometer on 5 March 2000; (b) the POAM III satellite instrument between 1 January and 20 March 2000; and (c) ozonesondes between 1 January and 30 March 2000. The profiles in Figures 12b and 12c represent vortex averages for 10 days centered on the indicated day of the year. The profile of O_3* (thin black line), the abundance of O_3 expected in the absence of any chemical loss, is estimated in Figure 12a by mapping the initial O_3 versus N_2O relation shown in Figure 5 onto a profile for N_2O measured by the balloon-borne LACE gas chromatograph in the core of the vortex on 5 March 2000 (see *Salawitch et al.* [2002] for details). Profiles of O_3* in Figures 12b and 12c are calculated by allowing the vortex average O_3 profiles from POAM III (see *Hoppel et al.* [2002] for details) and ozonesondes, respectively, to descend by amounts based on cooling rates from the SLIMCAT model (for this calculation, the mixing ratio of O_3 is assumed to be conserved during descent and is converted to concentration in the last step). All profiles are shown for the altitude and pressure the air would have been at on the date of the last measurement by each instrument. Profiles of O_3 and O_3* from the sondes, appropriate for the date indicated on each panel, are represented in the top two panels by gray solid lines. A second profile for O_3 from the sondes (gray dashed line) is given in Figure 12a, representing an average profile on 5 March 2000 for air in the core of the vortex.

Table 1. Comparisons of Chemical Loss of Column Ozone, Column $[O_3^*\text{-}O_3]$, Inside the Arctic Vortex for Winter 1999/2000 as Indicated by Date

Data Source	OMS Balloon	POAM III Satellite	Ozonesondes
Method	tracer-tracer (O_3 versus N_2O)	vortex-averaged descent	Match trajectory analysis
Reference	*Salawitch et al.* [2001]	*Hoppel et al.* [2001]	this paper
5 March 2000	61 ± 13 DU	51 ± 11 DU	53 ± 11 DU
15 March 2000	na	67 ± 11 DU	71 ± 12 DU
28 March 2000	na	na	88 ± 13 DU

as of 15 March based on the POAM III observations. The sonde observations and Match yield column $[O_3^*\text{-}O_3]$ = 75 DU and column $[O_3^*\text{-}O_3]$ = 71 ± 12 DU, respectively, for this date, in good agreement with the satellite value. The good agreement between each of these estimates of column loss of O_3 due to chemistry increases our confidence in the validity of each approach.

[30] Ozonesonde observations (Figure 12c) reveal that significant loss of ozone occurred in the Arctic vortex during the winter of 1999/2000 after it was last sampled by the OMS balloons, by the ER-2, and by POAM III. Between early January and late March, column $[O_3^*\text{-}O_3]$ equaled 87 DU based on the vortex-averaged sonde data in Figure 12c. The value for column $[O_3^*\text{-}O_3]$ from the Match approach (Figure 6c) is 88 ± 13 DU for the same date. Although both estimates of column $[O_3^*\text{-}O_3]$ are based on the same sonde data, they have been calculated in entirely different ways. As noted above, the Match approach is designed to minimize the effects of mixing on the estimated loss. The vortex average approach might, in theory, be affected by flow of air across the edge of the vortex. The good agreement between these two estimates of column $[O_3^*\text{-}O_3]$ further demonstrates that, for the winter of 1999/2000, transport of extravortex air did not play a significant role in altering the ozone content of the vortex.

[31] The analysis presented here shows that the amount of ozone destroyed by chemistry throughout the column during the Arctic winter of 1999/2000 amounted to 117 ± 14 DU by late March. Chemical processes, in combination with dynamical effects, led to 88 ± 13 DU reduction in the column abundance of O_3 that would have been present in the absence of any chemical loss during late March. The actual column abundance of O_3 in the Arctic vortex was 340 ± 30 DU in late March. In the absence of chemical loss, the column abundance in late March would have been ~430 DU if the motions of air were unchanged.

7. Conclusion

[32] Results from the SOLVE/THESEO 2000 field campaign show that the Arctic vortex during the winter of 1999/2000 was characterized by low temperatures, widespread PSCs, elevated ClO, and considerable chemical loss of ozone. Between early January and late March, loss of 70% of the initial abundance of O_3 occurred in a ~1 km layer near 18 km altitude. This is the largest local loss of ozone ever reported for the Arctic. Loss of more than 50% of initial O_3 occurred over a 3 km broad region. Chemistry alone destroyed 117 ± 14 DU of ozone in the column. Chemistry, in combination with dynamical effects, led to a reduction in the column abundance of ozone by 88 ± 13 DU (~26% of the observed column abundance of O_3 in March 2000) compared to the amount of O_3 that would have been present without chemistry, if the motions of air were unchanged.

[33] **Acknowledgments.** We thank the THESEO 2000 core group, the SOLVE project scientists, and all personnel associated with the project management for making this campaign possible. We thank the innumerable people that made this study possible due to their dedication: the ground staff at the ozonesonde stations and at ESRANGE, the ER-2 and DC-8 personnel, and the ER-2 and DC-8 pilots. We thank the European Centre for Medium-Range Weather Forecasts for supplying the meteorological data. The ozonesondes used in THESEO 2000 were supported through the EC Environment Programme under contracts EVK2-CT-1999-00047 and through numerous national projects. The SOLVE effort was supported by the Upper Atmospheric Research Program, the Atmospheric Chemistry, Modeling and Analysis Program, and the Atmospheric Effects of Aviation Program of the U.S. National Aeronautics and Space Administration. The POAM III experiment is supported by the U.S. Office of Naval Research and NASA. Research at the Jet Propulsion Laboratory, California Institute of Technology, is performed under contract with the U.S. National Aeronautics and Space Administration. Work at the Alfred Wegener Institute was supported by the BMBF under the project 07ATC08.

References

Austin, J., N. Butchart, and K. Shine, Possibility of an Arctic ozone hole in a doubled-CO_2 climate, *Nature*, *360*, 221–225, 1992.

Becker, G., R. Müller, D. S. McKenna, M. Rex, and K. S. Carslaw, Ozone loss rates in the Arctic stratosphere in the winter 1991/1992: Model calculations compared with Match results, *Geophys. Res. Let.*, *25*, 4325–4328, 1998.

Becker, G., R. Müller, D. S. McKenna, M. Rex, K. S. Carslaw, and H. Oelhaf, Ozone loss rates in the Arctic stratosphere in the winter 1994/1995: Model simulations underestimate results of the Match analysis, *J. Geophys. Res.*, *105*, 15,175–15,184, 2000.

Bevilacqua, R. M., C. P. Aellig, and J. E. Rosenfield, POAM II ozone observations in the Antarctic ozone hole in 1994, 1995, and 1996, *J. Geophys. Res.*, *102*, 23,643–23,658, 1997.

Beyerle, G., R. Neuber, O. Schrems, F. Wittrock, and B. Knudsen, Multiwavelength lidar measurements of stratospheric aerosols above Spitsbergen during winter 1992/1993, *Geophys. Res. Lett.*, *21*, 57–60, 1994.

Bremer, H., M. von König, A. Kleinböhl, H. Küllmann, K. Künzi, K. Bramstedt, J. P. Burrows, K.-U. Eichmann, M. Weber, and A. P. H. Goede, Ozone depletion observed by Airborne Submillimeter Radiometer during the Arctic winter 1999/2000, *J. Geophys. Res.*, *107*, 10.1029/2001JD000546, in press, 2002.

Chipperfield, M. P., Multiannual simulations with a three-dimensional chemical transport model, *J. Geophys. Res.*, *104*, 1781–1806, 1999.

Chipperfield, M. P., and R. L. Jones, Relative influence of atmospheric chemistry and transport on Arctic ozone trends, *Nature*, *400*, 551–554, 1999.

Greenblatt, J. B., et al., Defining the polar vortex edge from an N_2O: potential temperature correlation, *J. Geophys. Res.*, *107*, 10.1029/2001JD000575, in press, 2002a.

Greenblatt, J. B., et al., Tracer-based determination of vortex descent in the 1999/2000 Arctic winter, *J. Geophys. Res.*, *107*, 10.1029/2001JD000937, in press, 2002b.

Hansen, G., T. Svenoe, M. P. Chipperfield, A. Dahlback, and U.-P. Hoppe, Evidence of substantial ozone depletion in winter 1995/1996 over northern Norway, *Geophys. Res. Lett.*, *24*, 799–802, 1997.

Hanson, D. R., and K. Mauersberger, Laboratory studies of the nitric acid trihydrate: Implications for the south polar stratosphere, *Geophys. Res. Lett.*, *15*, 855–858, 1988.

Hofmann, D. J., and T. Deshler, Evidence from balloon measurements for chemical depletion of stratospheric ozone in the Arctic winter of 1989–90, *Nature*, *349*, 300–305, 1991.

Hoppel, K., R. M. Bevilacqua, G. Nedoluha, C. Deniel, F. Lefevre, J. D.

Lumpe, M. D. Fromm, C. E. Randall, J. E. Rosenfield, and M. Rex, POAM III observations of arctic ozone loss for the 1999/2000 winter, *J. Geophys. Res.*, *107*, 10.1029/2001JD000476, in press, 2002.

Knudsen, B., et al., Ozone depletion in and below the Arctic vortex for 1997, *Geophys. Res. Lett.*, *25*, 627–630, 1998.

Lucke, R. L., et al., The Polar Ozone and Aerosol Measurement (POAM) III instrument and early validation results, *J. Geophys. Res.*, *104*, 18,785–18,799, 1999.

Manney, G. L., et al., Chemical depletion of ozone in the Arctic lower stratosphere during winter 1992–93, *Nature*, *370*, 429–434, 1994.

Michelsen, H. A., G. L. Manney, M. R. Gunson, and R. Zander, Correlations of stratospheric abundances of NO_y, O_3, N_2O, and CH_4 derived from ATMOS measurements, *J. Geophys. Res.*, *103*, 2777–2780, 1998.

Müller, R., et al., Severe chemical ozone loss in the Arctic during the winter of 1995–1996, *Nature*, *389*, 709–712, 1997.

Pierson, J. M., et al., An investigation of ClO photochemistry in the chemically perturbed Arctic vortex, *J. Atmos. Chem.*, *32*, 61–81, 1999.

Plumb, R. A., D. W. Waugh, and M. P. Chipperfield, The effects of mixing on tracer relationships in the polar vortices, *J. Geophys. Res.*, *105*, 10,047–10,062, 2000.

Proffitt, M. H., et al., Ozone loss in the Arctic polar vortex inferred from high altitude aircraft measurements, *Nature*, *347*, 31–36, 1990.

Ray, E. A., F. L. Moore, J. W. Elkins, D. F. Hurst, P. A. Romashkin, G. S. Dutton, and D. W. Fahey, Descent and mixing in the 1999/2000 northern polar vortex inferred from in situ tracer measurements, *J. Geophys. Res.*, *107*, 10.1029/2001JD000961, in press, 2002.

Rex, M., et al., Prolonged stratospheric ozone loss in the 1995–96 Arctic winter, *Nature*, *389*, 835–838, 1997.

Rex, M., et al., In situ measurements of stratospheric ozone depletion rates in the Artic winter 1991/1992: A Lagrangian approach, *J. Geophys Res.*, *103*, 5843–5853, 1998.

Rex, M., et al., Chemical ozone loss in the Arctic winter 1994/95 as determined by the Match technique, *J. Atmos. Chem.*, *32*, 35–39, 1999.

Rex, M., et al., Arctic and Antarctic ozone layer observations—Chemical and dynamical aspects of variability and long-term changes in the polar stratosphere, *Polar Res.*, *19*(2), 193–204, 2000.

Richard, E. C., K. C. Aikin, A. E. Andrews, B. C. Daube, C. Gerbig, S. C. Wofsy, P. A. Romashkin, D. F. Hurst, E. A. Ray, and F. L. Moore, Severe chemical ozone loss inside the Arctic polar vortex during winter 1999–2000 inferred from in situ airborne measurements, *Geophys. Res. Lett.*, *28*, 2197–2200, 2001.

Salawitch, R. J., et al., Chemical loss of ozone in the Arctic polar vortex in the winter of 1991–92, *Science*, *261*, 1146–1149, 1993.

Salawitch, R. J., et al., Chemical loss of ozone during the Artic winter of 1999/2000: An analysis based on balloon-borne observations, *J. Geophys. Res.*, *107*, 10.1029/2001JD000620, in press, 2002.

Santee, M. L., G. L. Manney, N. J. Livesey, and J. W. Waters, UARS Microwave Limb Sounder observations of denitrification and ozone loss in the 2000 Arctic late winter, *Geophys. Res. Lett.*, *27*, 3213–3216, 2000.

Schoeberl, M. R., et al., Stratospheric constituent trends from ER-2 profile data, *Geophys. Res. Lett.*, *17*, 469–472, 1990.

Shindell, D. T., D. Rind, and P. Lonergang, Increased polar stratospheric ozone losses and delayed eventual recovery owing to increasing greenhouse-gas concentrations, *Nature*, *392*, 589–592, 1998.

Sinnhuber, B.-M., et al., Large loss of total ozone during the Arctic winter of 1999/2000, *Geophys. Res. Lett.*, *27*, 3473–3476, 2000.

Solomon, S., Stratospheric ozone depletion: A review of concepts and history, *Rev. Geophys.*, *37*, 275–316, 1999.

Vömel, H., D. W. Toohey, T. Deshler, and C. Kroger, Sunset observations of ClO in the arctic polar vortex and implications for ozone loss, *Geophys. Res. Lett.*, *28*, 4183–4186, 2001.

von der Gathen, P., et al., Observational evidence for chemical ozone depletion over the Arctic winter 1991–92, *Nature*, 375, 1995.

Woyke, T., et al., A test of our understanding of the ozone chemistry in the Arctic polar vortex based on in situ measurements of ClO, BrO, and O_3 in the 1994/1995 winter, *J. Geophys Res.*, *104*, 18,755–18,768, 1999.

H. Deckelmann, R. Neuber, M. Rex, A. Schulz, and P. von der Gathen, Alfred Wegener Institute for Polar and Marine Research, P.O. Box 600149 D-14401 Potsdam, Germany. (hdec@AWI-Potsdam.de; neuber@awi-potsdam.de; mrex@awi-Potsdam.de; aschulz@AWI-Potsdam.de; gathen@AWI-Potsdam.de)

J. Flesch, R. L. Herman, J. J. Margitan, R. J. Salawitch, G. D. C. Scott, B. Sen, C. G. C. Toon, and R. Webster, Jet Propulsion Laboratory, California Institute of Technology, 4800 Oak Grove Drive, Pasadena, CA 91109, USA. (gregory.j.flesch@jpl.nasa.gov; rherman@igor.jpl.nasa.gov; jjm@caesar.jpl.nasa.gov; rjs@caesar.jpl.nasa.gov; dcscott@igor.jpl.nasa.gov; bhaswar.sen@jpl.nasa.gov; toon@mark4sun.jpl.nasa.gov; chris.r.webster@jpl.nasa.gov)

N. R. P. Harris, European Ozone Research Coordinating Unit, 14 Union Road, Cambridge CB2 1HE, UK. (neil.harris@atm.ch.cam.ac.uk)

B. R. Bojkov and G. O. Braathen, NILU, Instituttveien 18, P.O. Box 100, N-2007 Kjeller, Norway. (bojan@nilu.no; geir@nilu.no)

M. Chipperfield and B.-M. Sinnhuber, University of Leeds, Leeds, LS2 9JT, UK. (martyn@lec.leeds.ac.uk; bms@env.leeds.ac.uk)

R. Alfier and E. Reimer, Meteorological Institute, FU Berlin, C.-H.-Becker Weg 6-10, D-12165 Berlin, Germany. (alfier@strat25.met.fu-berlin. de; reimer@zedat.fu-berlin.de)

R. Bevilacqua and K. Hoppel, Naval Research Laboratory, Code 7220, Washington, D.C. 20375, USA. (bevilacq@poamb.nrl.navy.mil; hoppel@poamb.nrl.navy.mil)

M. Fromm and J. Lumpe, Computational Physics, Inc., 8001 Braddock Road, Springfield, VA 22151, USA. (fromm@poama.nrl.navy.mil; lumpe@cpi.com)

H. Bremer, A. Kleinböhl, H. Küllmann, K. Künzi, and M. von König, Institute of Environmental Physics, University of Bremen, P.O. Box 330 440, D-28334 Bremen, Germany. (holger@clox.physik.uni-bremen.de; kleinb@clox.physik.uni-bremen.de; harry@schalk.physik.uni-bremen.de; kunzi@physik.uni-bremen.de; miriam@iup.physik.uni-bremen.de)

D. Toohey, Program in Atmospheric and Oceanic Science, University of Colorado, Boulder, PAOS/311 UCB, Boulder, CO 80309, USA. (toohey@colorado.edu)

H. Vömel, Cooperative Institute for Research in Environmental Sciences (CIRES), Campus Box 216, University of Colorado, Boulder, CO 80309, USA. (hvoemel@cmdl.noaa.gov)

K. Aikin, J. W. Elkins, D. F. Hurst, F. L. Moore, E. A. Ray, E. Richard, and P. Romashkin, National Oceanic and Atmospheric Administration, Boulder, CO 80303, USA. (aikin@al.noaa.gov; jelkins@cmdl.noaa.gov; dhurst@cmdl.noaa.gov; fmoore@cmdl.noaa.gov; eray@cmdl.noaa.gov; richard@al.noaa.gov; promashkin@cmdl.noaa.gov)

H. Jost, J. B. Greenblatt, M. Loewenstein, and J. R. Podolske, NASA Ames Research Center, Moffett Field, CA 94035, USA. (hjost@mail.arc.nasa.gov; jgreenblatt@mail.arc.nasa.gov; mloewenstein@mail.arc.nasa.gov; jpodolske@mail.arc.nasa.gov)

P. Wennberg, Division of Geological and Planetary Sciences, California Institute of Technology, Pasadena, CA 91125, USA. (wennberg@gps.caltech.edu)

M. Allart, KNMI, P.O. Box 201, N-3730 AE De Bilt, Netherlands. (allaart@knmi.nl)

H. Claude, DWD, Observatory Hohenpeißenberg, Albin-Schwaiger-Weg 10, D-82383 Hohenpeißenberg, Germany. (claude@mohp.dwd.d400.de)

J. Davies and H. Fast, Atmospheric Environment Service, 4905 Dufferin Street, Downsview, ON, M3H 5T4, Canada. (jonathan.davies@ec.gc.ca; hans.fast@ec.gc.ca)

W. Davies, Department of Physics, University of Wales, Aberystwyth, SY23 3BZ Wales, UK. (wdd@aber.ac.uk)

H. de Backer, Royal Meteorological Institute, Ringlaan 3, B-1180 Brussels, Belgium. (hugo@oma.be)

H. Dier, Meteorologisches Observatorium Lindenberg, D-15864 Lindenberg, Germany. (dier@mol.dwd.d400.de)

V. Dorokhov, CAO, Pervomajskaya Street 3, Dolgoprudny, Moscow Region, 141700, Russia. (vdor@ozone.mipt.ru)

Y. Kondo, Research Center for Advanced Science and Technology, University of Tokyo, 4-6-1 Komaba, Meguro, Tokyo 153-8904, Japan. (kondo@atmos.rcast.u-tokyo.ac.jp)

E. Kyrö, MWM, Centre of Aerology, Zegrzynska Str. 38, 05-119 Legionowo, Poland. (esko.kyro@fmi.fi)

Z. Litynska, Institute of Meteorology and Water Management, Centre of Aerology, Zegrzynska Str. 38, 95-119 Legionowo, Poland. (zenoblit@pol.pl)

I. S. Mikkelsen, Danish Meteorological Institute, Lyngbyvej 100, DK-2100 Copenhagen Oe, Denmark. (ism@dmi.min.dk)

M. J. Molyneux, UK Met Office OP2C, London Road, Bracknell, Berkshire, RG11 2SZ, UK. (mjmolyneux@meto.gov.uk)

E. Moran and V. Yushkov, IMS, Valentia Observatory, Cahirciveen, Co. Kerry, Ireland. (eoinm@valentia.iol.ie; vvcao@ozone.mipt.ru)

T. Nagai, Meteorological Research Institute, 1-1, Nagamine, Tsukuba, Ibaraki 305-0052, Japan. (tnagai@mri-jma.go.jp)

H. Nakane, National Institute for Environmental Studies, 16-2 Onogawa, Tsukuba, Ibaraki 305-0053, Japan. (nakane@nies.go.jp)

C. Parrondo, INTA, Torrejon de Argoz, Madrid, Spain. (parrondosc@inta.es)

F. Ravegnani, C.N.R. Fisbat Institute, Via Gobetti 101, Bologna, Italy. (fabrizio@o3.fisbat.bo.cnr.it)

P. Skrivankova, Czech Hydrometical Institute, Na Sabatce 17, 14306 Prague, Czech Republic. (skrivankova@chmi.cz)

P. Viatte, SMI, Les Invuardes, CH-1530 Payerne, Switzerland. (pvi@sap.sma.ch)